Rapid Measurements and Mapping of Tracer Gas Concentrations in a Large Indoor Space

Marc L Fischer[*], Phillip N Price, Tracy L Thatcher, Carrie A Schwalbe, Mathias J Craig, Emily E Wood, Richard G Sextro, and Ashok J Gadgil

Indoor Environment Department, Environmental Energy Technologies Division, Ernest Orlando Lawrence Berkeley National Laboratory, Berkeley, CA, 94720

ABSTRACT

Rapid mapping of gas concentrations in air benefits studies of atmospheric phenomena ranging from pollutant dispersion to surface layer meteorology. Here we demonstrate a technique that combines multiple-open-path tunable-diode-laser (TDL) spectroscopy and computed tomography to map tracer gas concentrations with approximately 0.5 m spatial and 7 second temporal resolution. Releasing CH_4 in a large (7m x 9m x 11m high) ventilated chamber, we measured path-integrated CH_4 concentrations over a planar array of 28 "long" (2-10 m) optical paths, recording a complete sequence of measurements every 7 seconds during the course of hour-long experiments. Maps of CH_4 concentration were reconstructed from the long-path data and compared with simultaneous measurements from 28 "short" (0.5 m) optical paths. On average, the reconstructed maps capture ~ 74% of the variance in the short path measurements. The accuracy of the reconstructed maps is limited, in large part, by the number of optical paths and the time required for the measurement. Straightforward enhancements to the instrumentation will allow rapid mapping of three-dimensional gas concentrations in indoor and outdoor air, with sub-second temporal resolution.

[*] Address and email of corresponding author:

Bldg 90-3058

Environmental Energy Technologies Division

Ernest Orlando Lawrence Berkeley National Laboratory

1 Cyclotron Rd.

Berkeley, CA 94720

MLFischer@lbl.gov

INTRODUCTION

Measurements of tracer gas dispersion are useful as a means for quantifying atmospheric transport. Research activities in a broad range of fields benefit from this capability. Examples include flow visualization measurements of gas dispersion in large indoor or outdoor spaces. Such measurements can provide experimental verification of computational models of pollutant dispersion, or footprint models of ecosystem-atmosphere trace gas exchange. For many of these phenomena, the spatial and temporal scales of interest range from 0.1 to 10000 meters and 0.1 to 10000 seconds. The smallest scales might correspond to that of a personal breathing zone or turbulent eddies, the mid range scales to ventilation and mixed convection in buildings, and the largest scales to turbulent transport in the atmospheric surface boundary layer.

In outdoor applications, technical considerations have generally restricted the temporal resolution of previous mapping measurements to many minutes or hours. Exceptions are LIDAR measurements of atmospheric water vapor, which can be obtained over distances up to kilometers with approximately 1.5 m spatial and 0.3 second temporal resolution along a single line of sight (Cooper et al., 1994; Eichinger et al., 1999). Sequential measurements over many lines of sight are used to generate maps. LIDAR measurements are particularly well suited for outdoor measurements on large spatial scales because scattering of the laser radiation by aerosols or gas species provides the return beam, eliminating the need for retro-reflectors commonly used with many open-path systems.

Previous work on measuring the dispersion of pollutants in indoor air has not, to our knowledge, probed time scales shorter than minutes. Techniques used for these measurements have included conventional pump and tube sampling (e.g. Baughman et al., 1994; Drescher et al., 1995), and open-path (OP) remote sensing, in combination with computed tomography (CT) (Yost et al., 1994; Drescher et al., 1996, 1997). Most of this work covered spatial scales on order of 1-20 m, with approximately 1 meter spatial and 100-1000 second temporal resolution. Here the temporal and spatial resolution was limited for pump-and-tube sampling by the time required to switch valves and collect samples from some number of locations, and for OP-CT by the time to sequentially measure many overlapping beam paths with a Fourier Transform Infrared (FTIR) spectrometer. While the temporal resolution of these systems has been modest, they can detect a broad range of compounds and are hence an attractive for monitoring of unknown pollutants.

Here, we describe a system for mapping concentrations a tracer gas with 7 second temporal and approximately 0.5 m spatial resolution. The system rapidly measures path-integrated gas concentrations over many open paths that are defined by a source of radiation and a detector. The measured data are then used to reconstruct a map of gas concentration using computed tomography.

MATERIALS and METHODS

This section describes the gas measurement system, the chamber used for the experiments, the initial tests of the system, and the mapping experiments. Additional details concerning this system and the overall experimental program can be found in Gadgil et al. (2000).

Tracer Gas Measurement System

Path-integrated methane (CH_4) concentrations are determined by measuring the near-infrared absorption spectrum of CH_4 gas at a wavelength near 1.65 micrometers using a commercially available (Unisearch Assoc. Inc.), fiber-optic based, tunable diode laser spectrometer, termed LasIR (Schiff et al.,1999). The LasIR measures the absorption spectrum using two-tone frequency modulation (TTFM). For a review of modulation techniques see Brassington (1995). For this application, TTFM offers an advantage over other modulation techniques in that high signal to noise measurements can be obtained using a diode laser and relatively inexpensive gallium phosphide detectors, all operated near room temperature. The resulting detection limit for CH_4 in ambient air is approximately 2 ppm-m in a one second integration.

In our application, the LasIR is configured to measure two open path channels simultaneously. An optical layout of the spectrometer and the multiplexers is shown in Figure 1. Following the radiation path from the laser to a photodiode detector, first a beam splitter diverts 10% of the radiation to an internal CH_4 reference channel made up of a sealed cell containing ~ 1 % CH_4 and a detector. Second, the remaining radiation is passed through a calibration cell and then divided into two equal parts by a second beam splitter. Third, in order to obtain measurements over many open paths, the two beams are sent to two 32 channel communication-grade beam switches (JDS, Fitel Inc.). Each switch supplies radiation to one of up to 32 sets of open-path optics. Each set of open-path optics contains a lens that collimates the radiation emitted by the optical fiber, receiving optics, and a photodiode detector. All of the fiber-optic connectors have angled surfaces to reduce interference fringes that are due to multiple internal reflections within the optical paths. Finally, the electrical signals from the two detectors being illuminated with laser radiation at a given moment are returned to the LasIR over coaxial cable using two 32 channel radio-frequency (RF) multiplexers.

As shown in Figure 1, the open-path optics for this system are configured for two path ranges of path legnths. First "long" optical paths (from 2 to 30 m in path length) are defined by sets of physically separated source and receiving optics. The source collimates the radiation emerging from the optical fiber using a single 0.6 cm diameter glass lens that has been anti-reflection coated for 1.6 micrometer wavelength radiation. The receiving optics are a 2.5 cm diameter collection lens that has no anti-reflection coating and a 0.3 cm diameter glass lens that is part of the GAP-1000L detector package (Germanium Devices Inc.). Both the source and receiving optics are alligned using mirror mounts that allow limited adjustment of the direction of the optic axis. Coarse positioning of the long path optics is achieved with a pair of right angle rods with clamps (source optics) or ball and socket (receiver optics) mounts.

Second, "short" optical paths (each 0.1-1 m in length) are defined by pairs of co-mounted source and receiving optics. Here, the optics are comprised of a source optic that is the same as for the long paths, a folding mirror, and only the lens on a GAP-1000L detector. Each of the short path components is aligned using a two-axis mirror mount. The mounts are positioned along a common rod using right angle rod and clamp fixtures. In the standard configuration the optical mounts are 0.5 m apart, yielding an physical length of 0.5 m and an optical path length of 1 m.

A host computer, running software written by Unisearch Assoc. Inc., controls the optical switches and RF multiplexers to select which long and short paths will be measured, and acquires

3

the measured data from the LasIR. Data from the two channels of the LasIR are transmitted to the host computer at 83 Hz using two 16-bit parallel digital interfaces. The 83 Hz binary data can be recorded if desired. The host computer also averages the binary data over a specified integration interval, applies calibration factors stored in a calibration file, and displays and stores the averaged data. For the experiments described below, the multiplexers are switched to a new path every 200 msec, allowing approximately 170 msec for measurement and a 30 msec settling time per path. The time required to complete a measurement sequence consisting of sequential measurements of 30 open paths on each multiplexer is 7 seconds, after including approximately 1 second for the multiplexers to reset.

Instrument Calibration

The offset and gain of each open path are determined by measuring the signals obtained when the 12 cm long calibration cell is filled first with N_2 and then with 1% CH_4 in N_2. The offset signals are measured when the cell is filled with N_2. The offset signal is the sum of the instrument offset and the path integrated CH_4 concentration in the chamber (ambient air typically contains ~ 2 ppm CH_4). The gain is determined from the measured increase in signal above the offset when the cell is filled with 1% CH_4 in N_2 (equivalent to a path integrated signal of 1200 ppm-m). The calibration sequence is typically performed at the beginning of a series of experiments to set the calibration factors used for real-time display of the measured data. The calibration is also repeated at the beginning of each individual mapping experiment to record offsets due to residual CH_4 present in the chamber from previous experiments.

Before the mapping experiments, we also check the linearity of the system by measuring calibration signals using two additional gas standards of 0.1% and 4% CH_4. Based on these measurements, the gains of all open paths are within 5% of that measured with the standard two point (N_2, and 1% CH_4) calibration, over a range of path-integrated CH_4 concentrations from 120 to 4800 ppm-m.

Experimental Chamber and Tracer Gas Release System

As shown in Figure 2, the experimental chamber has the approximate dimensions of 7 m x 9 m x 11 m in height (~ 690 m^3 volume), which is sufficiently tall that one can study mixed convection relevant for other large indoor spaces. The chamber is lined with galvanized steel, as it was originally used as an electromagnetically shielded room for high voltage electronics. We sealed the sheet seams with aluminum tape and estimate the overall air leakage rate to be approximately 1 air change per hour under average conditions. The floor, the lower 2.3 m of the chamber walls, and the entire east wall of the chamber are constructed of concrete. The remaining upper sections of the chamber walls and ceiling are of standard wood-frame construction.

A dedicated heating and ventilation (HVAC) system supplies air to the room at temperatures controllable to 0.5 C in a range from approximately 10 to 30 C. The total flow rate and relative amounts of outdoor air and re-circulated air supplied to the room can be adjusted from approximately 1.5 to 6 air changes per hour (ACH). The total flow rate is measured with approximately 5 % accuracy using 15 cm and 30 cm diameter flow venturis, each instrumented with a digital manometer. In addition to the HVAC system, a blower mounted in the south wall of the chamber at a height of approximately 4 m can be used to rapidly flush the chamber. The

five supply registers, shown in Figure 2, are each 1.3 m wide and 0.3 m high. The exhaust register is a square approximately 50 cm on a side mounted in the ceiling.

Tracer gas (4% CH_4 in N_2) is released at a controlled rate into the room from a 1m x 1m area source using a mass flow controller (Sierra Inst. Inc.). The tracer is released approximately uniformly over the source area from a 0.8 mm diameter tube wound in a spiral which, in turn, is contained within a 1 m x 1 m x 0.05 m high box with a perforated cover. The radial distance between consecutive turns of the spiral is approximately 20 cm. The tube has 1.2 mm diameter holes drilled at 10 cm intervals. The release rate is controlled with a mass flow controller. In all of the release experiments described in this paper the source is located 0.5 m above the floor, at the position shown in Figure 3.

Location and Mounting of the Open-path Optics

For the experiments described here, we deployed 28 long paths and 28 short paths in a horizontal plane 2 m above the chamber floor. A plan view of the optical path layout is shown in Figure 3. The long paths are arranged in four overlapping groups of parallel rays. The groups are arranged at angles of 0, 45, 90, and 145 degrees. This relatively simple geometry was chosen because computational tests using tomographic reconstructions of synthetic data suggested it would obtain accurate maps (Gadgil et al., 2000). The long path optical sensors are mounted (using magnetic clamps) to 0.5 cm thick steel strips fixed to the chamber walls, while the short-path sensors are suspended from cables just above the plane defined by the long paths. In addition to the paths shown in Figure 3, an additional short path is mounted in an air supply register to monitor the concentration of CH_4 in the ventilation air supplied to the room.

Tomographic Reconstruction Algorithm

Path-integrated concentrations from the long path measurements are used as inputs to a 2-dimensional computated tomography algorithm that determines a best fit reconstructed concentration distribution in the measurement plane, using Smooth Basis Function Minimization (SBFM) (Drescher et al. 1996). SBFM is well suited for reconstructing gas concentrations because it generates smooth reconstructions with a small number of local concentration maxima, while still allowing large concentration gradients within the measurement domain.

This application of SBFM includes some minor changes to the previous work by Drescher et al. (1996), which are detailed in Gadgil et al. (2000). Briefly, the reconstructed gas concentration in the measurement plane is written as a superposition of 1 to 5 two-dimensional Gaussian peaks, each described by a position and rotation relative the coordinates of the room, two widths, and an amplitude. The program has three modules. The first module uses the algebraic reconstruction technique (ART; see Gordon et al., 1970) to determine approximate magnitudes and locations of the concentration peaks. These estimates are used as initial values in the second module, which uses simulated annealing (see e.g., Press et al., 1996) with adaptive step sizes to search for a global "best fit" set of Gaussian parameters. The third module applies a local gradient search to fine tune the parameters obtained by simulated annealing. When reconstructing data from sequential sets of optical scans, ART is used only to obtain initial parameter estimates for the first set; subsequently, the final parameter estimates from one time interval are used as inputs to the simulated annealing algorithm for the next time interval. Computations were performed using

the Mathematica (Wolfram Research Inc.) programming environment.   Reconstruction of one complete long-path measurement sequence (collected in 7 seconds) takes approximately 100 seconds on a 450 MHz Pentium PC.

CH_4 Release Experiments

Before conducting long-path measurements for mapping experiments, we first performed CH_4 mixing measurements as a combined test of the instrument calibration, tracer gas release system, and the volume and air-tightness of the experimental chamber. For this purpose, we released 0.032 m^3 of CH_4 into the chamber under well-mixed conditions, created by running an additional fan in the chamber in addition to the chamber HVAC systems set for full recirculation (no fresh air supplied from outside). The resulting mean CH_4 concentrations measured by the long (short) paths were approximately 10% (25%) higher than that expected, based on the estimated volume of CH_4 released, and the estimated chamber volume (0.032 m^3 /694 m^3 = 46 ppm). Of importance for estimating uncertainty in computed tomographic reconstructions, the range in concentrations for the short and long paths were all within 10% of their respective mean concentrations.

For each of the mapping experiments described here, we operated the chamber at a constant ventilation rate set between 0.5 and 1.2 m^3/s (6.4 ACH), with no recirculation of chamber air (100% outside air). In these tests we released tracer at a constant rate that allows us to examine transport and dispersion under steady flow conditions. At the beginning of each experiment we performed a 400 second calibration sequence to measure the offset and gain of the open paths. Following the calibration, we released the tracer at a rate of 0.6 liters (CH_4) per minute into the chamber over the period from 400 to 2600 seconds. After each experiment, the chamber was then flushed with outdoor air using a ventilation fan, in preparation for the next experiment. In this paper we examine the system performance for four experiments conducted at a common ventilation rate of 1.2 m^3/s.   In a future paper we will describe the effects of varied ventilation rate and the location of the tracer gas source on the characteristics of the gas dispersion. Figure 4 shows the path averaged CH_4 concentrations, measured over selected long and short paths, during one typical experiment. The path-to-path differences in the time at which the CH_4 appears, and the maximum concentration differences measured, are due to the different positions of the paths within the chamber. As can be seen, the concentration of CH_4 initially varies in both rapidly in time and across space as the tracer is transported within the chamber. Over time the concentrations grow toward a quasi-stationary values.

RESULTS and DISCUSSION

Maps of gas concentration are reconstructed using the 28 long path measurements from each complete measurement sequence (every 7 seconds).   This produces approximately 316 reconstructed maps, from the period when CH_4 was being released into the chamber times (from 400 to 2600 seconds). Figure 5 shows a sample of six reconstructed maps that illustrate how the pattern of gas concentrations within the measurement plane changed during the experiment shown in Figure 4. Despite the long duration of the experiment, the CH_4 concentration in the measurement plane does not reach a well-mixed state because advective flows of air maintain concentration gradients more effectively than turbulent diffusion can erase them. Figure 4 also

6

shows the CH_4 concentrations measured by each of the short paths. Visually, the agreement between reconstructed maps and short path measurements is generally quite good.

We quantitatively test the agreement between short path measurements and reconstructed maps by comparing the short path measurements with predicted path-integrated gas concentrations at the same locations, generated using the reconstructed maps. At each short path measurement location, the predicted concentration is obtained by integrating the corresponding reconstructed concentration over the length of that short path. We compare the measured and predicted path integrals using two measures.

First, we estimate the fraction of the spatial structure in the measured short path data that is captured in the reconstructed maps, by computing the linear regression of the 28 short path measurements on the 28 predicted integrals. The R^2 of the regression quantifies the fraction of the variance in the measured data that is captured by the fit and thus the degree to which spatial structures in the measured short path data are captured by the reconstruction. As an example, the Figure 6 a) shows the measured and predicted short path data from the measurement sequence beginning at time t = 2031 seconds of the experiment shown in Figure 5. Figure 6 b) shows all of data points from 400 to 2600 seconds; generally, the reconstructed maps capture a large fraction of the variance in the short-path measurements.

We summarize these results by computing quantiles of R^2 for each of four experiments that were performed under similar flow conditions. As shown in Table 1, the median values of R^2 for the four experiments are all in the range from 0.72 to 0.79, while 90% of the values exceed 0.45 to 0.66. The limitation of this measure is that it is not sensitive to differences in the average concentration or to the constant of proportionality between the measured and reconstructed concentrations, because R^2 is computed from the residuals to the fit after subtracting the best fit offset and a slope.

On average, the predicted short-path gas concentrations are approximately 10% higher than the short-path measurements for the experiment. This may occur, in part, because of a relative difference in the average gain of the short and long paths. Consistent with this observation, the average of measured long path concentrations for this experiment is about 10% higher that the average of measured short path concentrations. However, caution is necessary in interpreting the ratio of average concentrations as a precise measure of a difference in gain between the long and short paths, because the long paths observe parts of the measurement plane not covered by the short paths.

A second, more stringent measure of reconstruction quality is includes differences in offsets gains between the short and long paths. This second measure is calculated as the root mean squared (rms) deviation between measured and predicted short path integrals, normalized by the mean of the measured short path integrals:

$$f = \frac{\sqrt{\frac{1}{N}\sum\left(y_i^{meas} - y_i^{pred}\right)^2}}{\frac{1}{N}\sum y_i^{meas}},$$

where y_i^{meas} and y_i^{pred} are the measured and predicted short-path integrals for path i, and the sum is computed over the 28 short path measurements during a single 7 second measurement sequence.   From the approximately 316 measurement sequences from each of the four experiments, the median values of f range from 0.26 to 0.43, indicating rms errors of between 26 and 43% of the mean concentration. Generally, the larger normalized rms errors occur in the first 500 seconds of the experiment when the mean CH_4 concentrations are lower and are changing rapidly.

While the system performance is adequate for capturing most of the time varying features of the gas distribution, improvements in the spatial and temporal resolution are possible. First, the gas concentrations may have spatial structure small enough to be missed in all paths, or to be detected in a single long (or short) path but not be detected in nearby paths. Some solutions to this problem are to increase the spatial coverage by folding existing paths with mirrors, and to increase the spatial resolution by adding more paths. Second, temporal variations in the gas concentration can occur on time scales comparable to or shorter than the time required (currently 7 seconds) to complete a measurement sequence of all 28 long (or short) paths. In this case the measurement sequence can generate long-path data that do not correspond to a single stationary concentration map. The solutions to the problems of slow sequential measurements are to reduce measurement time and measure all paths simultaneously.   Toward this end, we are currently designing a new system that uses multiple lasers to measure 64 paths in 0.1 seconds.

CONCLUSION

We have demonstrated that tunable diode laser spectroscopy and computed tomography can be combined to accurately map tracer gas concentrations with approximately 0.5 m spatial and 7 second temporal resolution.   This represents a significant advance over previous methods for mapping tracer gas concentrations, enabling the examination of transient phenomena on time scales of seconds rather than minutes. At present, CT reconstruction is performed after the experiment is completed. However, the current measurement system could be used in combination with a new CT reconstruction algorithm described by Price et al. (2000) to measure and display concentration maps with 7 second resolution in real time.   Future improvements in the gas measurement system are expected to allow accurate measurement of advection and turbulence driven concentration variations, on sub-second time scales relevant for additional studies of air dispersion.

ACKNOWLEDGEMENTS

REFERENCES

Baughman, A. V., A. J. Gadgil and W. W. Nazaroff, 1994. *Mixing of a Point Source Pollutant By Natural Convection Flow Within a Room*. Indoor Air 4, 114-122.

Brassington, D. J., 1995. Tunable Diode Laser Absorption Spectroscopy for the Measurement of Atmospheric Species. Spectroscopy in Environmental Science. R. J. H. Clark, and R.E. Hester, John Wiley & Sons: 85-148.

Cooper, D. I., W. E. Eichinger, D. E. Hof, D. Seville-Jones, R. C. Quick and J. Tiee, 1994. Observations of coherent structures from a scanning lidar over an irrigated orchard. Agricultural and Forest Meteorology 67, 239-252.

Drescher, A. C., C. Lobascio, A. J. Gadgil and W. W. Nazaroff, 1995. Mixing of a Point-Source Indoor Pollutant By Forced Convection. Indoor Air 5, 285-285.

Drescher, A. C., A. J. Gadgil, P. N. Price and W. W. Nazaroff, 1996. Novel Approach For Tomographic Reconstruction of Gas Concentration Distributions in Air - Use of Smooth Basis Functions and Simulated Annealing. Atmospheric Environment 30, 929-940.

Drescher, A. C., D. Y. Park, M. G. Yost, A. J. Gadgil, S. P. Levine and W. W. Nazaroff, 1997. Stationary and time-dependent indoor tracer-gas concentration profiles measured by OP-FTIR remote sensing and SBFM-computed tomography. Atmospheric Environment 31, 727-740.

Eichinger, W. E., D. I. Cooper, P. R. Forman, J. Griegos, M. A. Osborn, D. Richter, L. L. Tellier and R. Thornton, 1999. The development of a scanning raman water vapor lidar for boundary layer and tropospheric observations. Journal of Atmospheric and Oceanic Technology 16, 1753-1766.

Gadgil, A.J., Finlayson, E.U., Fischer, M.L., Price, P.N., Thatcher, T.L., Craig, M., Hong, K.H., Housman, J., Schwalbe, C.A., Wilson, D., Wood J.E., and R. G. Sextro, 2000. Status Report January 2000: Investigating Dispersion of an Airborne Contaminant in a Large Space, LBNL Report 44791.

Gordon, R., Bender, R., and G.T. Herman, 1970. Algebraic reconstruction techniques ART for three dimensional electron microscopy and X-ray photography. Journal of Theoretical Biology 29, 471-481.

Press, W. H., Flannery, B. P., Teukolsky, S. A., and W. T. Vetterling, 1986 .   Numerical Recipes: The Art of Scientific Computing. Cambridge University Press, New York.

Price, P. N., Fischer, M. L., Gadgil, A. J., and R. G. Sextro, 2000. Algorithm for rapid gas concentration tomography. Lawrence Berkeley National Laboratory, report # 46236.

Schiff, H. I., A. Chanda, J. Pisano and G. Mackay, 1999. The LasIR-a tunable diode laser system for environmental and industrial applications. Proceedings of the SPIE - The International Society for Optical Engineering 3535, 132-40.

Yost, M. G., A. J. Gadgil, A. C. Drescher, Y. Zhou, M. A. Simonds, S. P. Levine, W. W. Nazaroff and P. A. Saisan, 1994. Imaging Indoor Tracer-Gas Concentrations With Computed Tomography - Experimental Results With a Remote Sensing FTIR System. American Industrial Hygiene Association Journal 55, 395-402.

Wu, C. F., M. G. Yost, R. A. Hashmonay and D. Y. Park, 1999. Experimental evaluation of a radial beam geometry for mapping air pollutants using optical remote sensing and computed tomography. Atmospheric Environment 33, 4709-4716.

TABLES

Table 1. Fraction of measurement sequences for four mapping experiments whose values of R^2 exceed the stated values. The R^2 values are computed from the linear regression between measured and predicted short-path concentrations for each of the measurement sequences conducted during the experiments.

Fraction	Experiment 1	Experiment 2	Experiment 3	Experiment 4
0.95	0.24	0.58	0.37	0.40
0.90	0.45	0.66	0.45	0.50
0.75	0.61	0.73	0.62	0.62
0.5	0.74	0.79	0.72	0.74
0.25	0.80	0.84	0.80	0.81
0.10	0.86	0.88	0.85	0.86
0.05	0.88	0.89	0.87	0.89

FIGURES
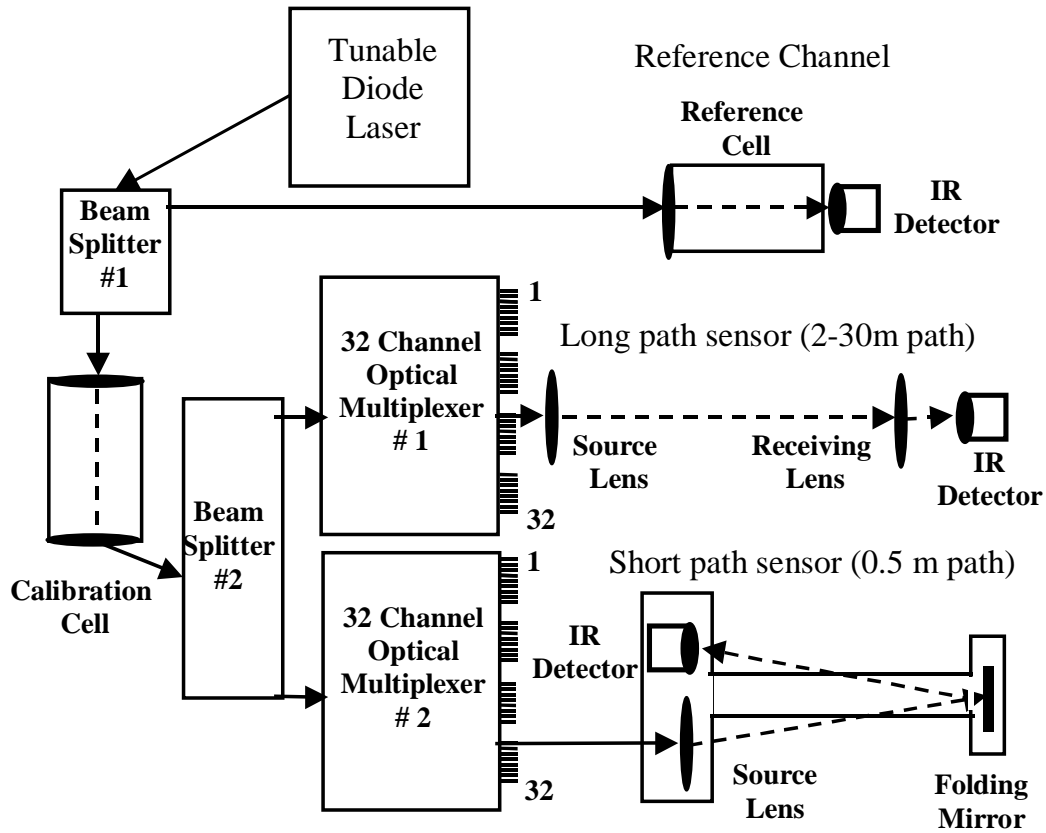
Figure 1 Optical layout of LasIR spectrometer and open-path optics. Solid lines indicate optical fiber. Dashed lines indicate open-paths.   Optics for one long path and one short path each are shown connected to one of the 32 possible outputs of optical multiplexers 1 and 2 respectively.
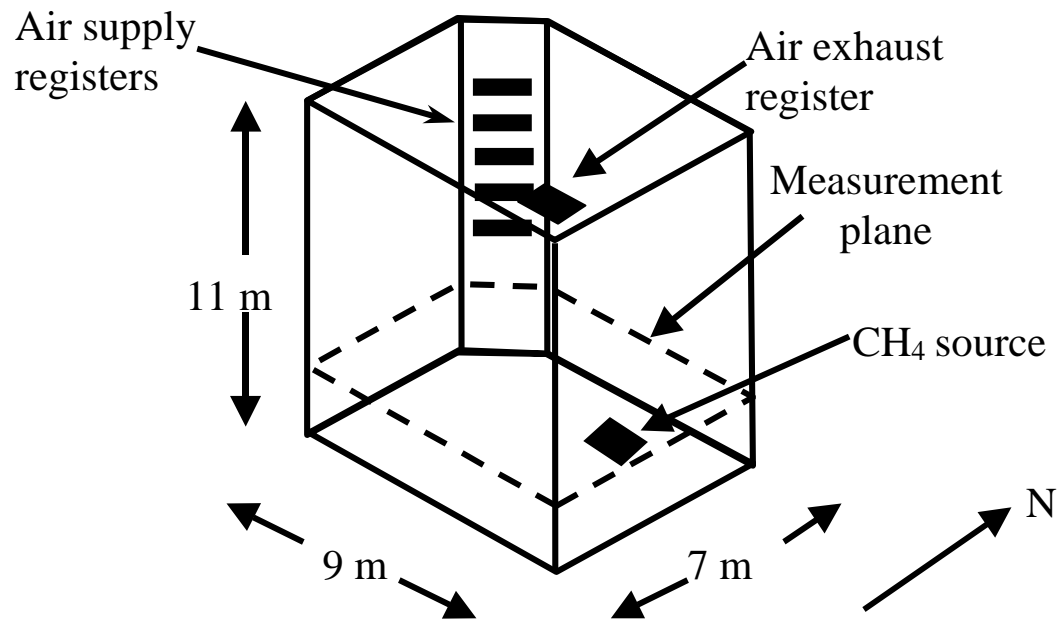
Figure 2 Perspective view of experimental chamber showing air supply and return registers, tracer gas release source, and open-path measurement plane. North is indicated by the arrow and "N" symbol.
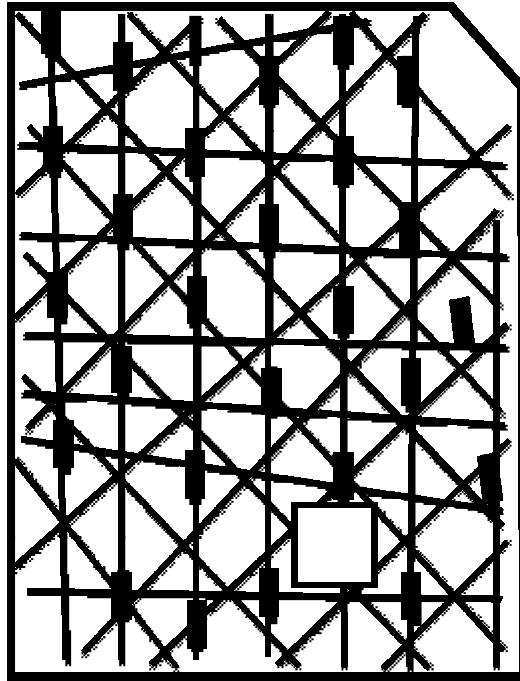
Figure 3 Plan view of measurement plane, showing the CH$_4$ source location (square), the 28 long paths (thin lines) used to calculate a computed reconstruction, and the 28 short paths (thick lines) used to check the quality of the reconstruction.   The triangle in the upper right corner shows the position of the air supply registers.
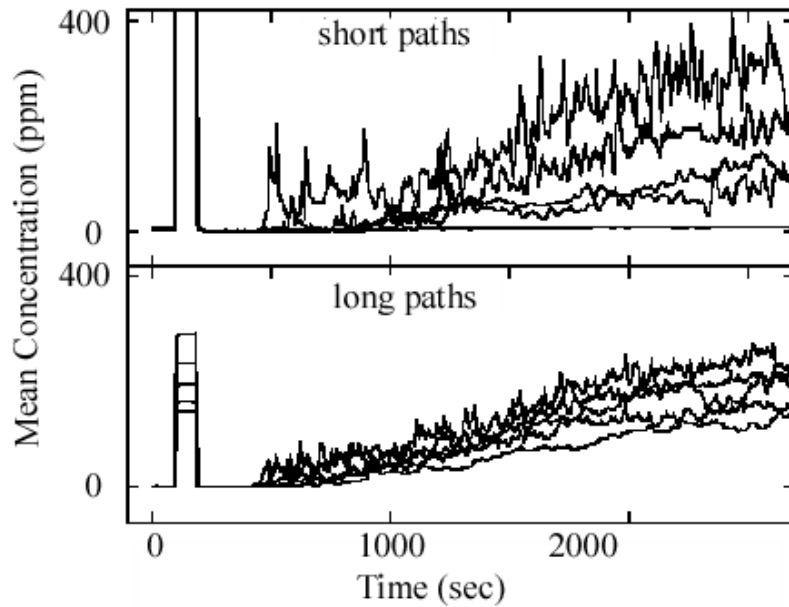
Figure 4 Path average CH$_4$ concentrations (path integrals normalized by path length) measured by selected short (upper panel) and long (lower panel) paths as a function of time during a CH$_4$ release experiment. The differences in average concentration observed by the different paths are due differing positions in the chamber. The short path with nearly constant low concentration was positioned above the measurement plane in a air supply register to monitor the CH$_4$ concentration in the air supplied to the chamber.
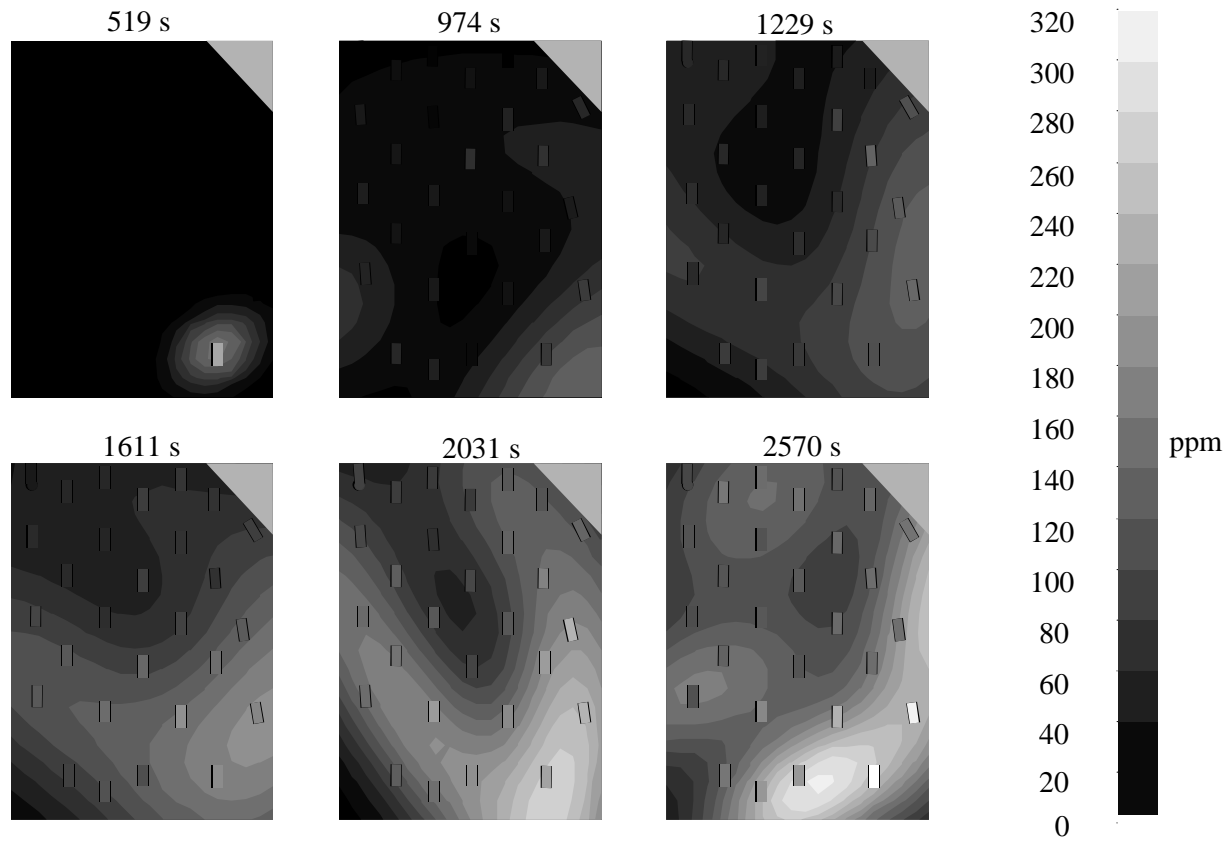
Figure 5 **Gas concentration maps reconstructed from data collected during a set of 7 second long measurement intervals starting at 519, 974, 1289, 1611, 2031, and 2570 seconds into the mapping experiment of Figure 4. The maps show the gradual development toward a quasi-stationary concentration field.**
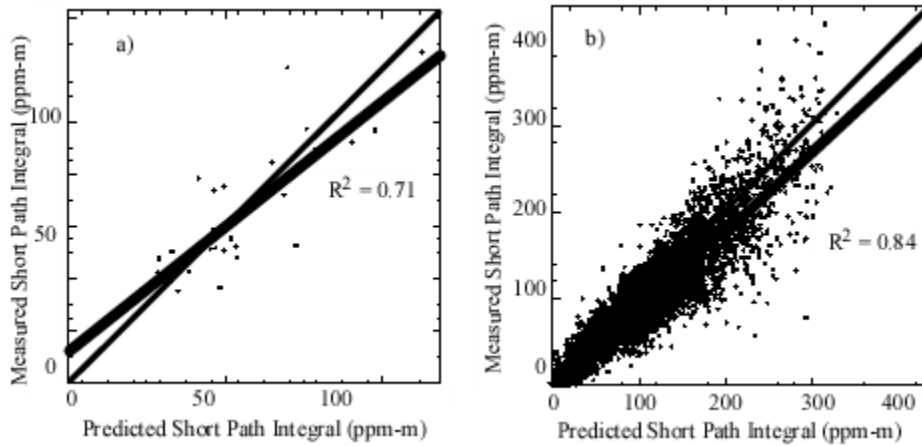
Figure 6 Comparison of measured short path concentrations and those predicted by integrating the short path over the reconstructed gas concentration from the mapping experiment shown in Figure 4. The 1:1 line (thin), the linear regression line (thick), and R^2 value of the regression are also shown. Panel a) shows the results for the 7 second measurement sequence collected starting at time, t = 1611; Panel b) shows all the data collected from 400 to 2600 seconds during experiment. On average, the predicted short path values are within 10% of the measured values.